Baryon Number, Strangeness and Electric Charge Fluctuations in QCD at High Temperature

M. Cheng[*a], P. Hegde[b,c] C. Jung[c], F. Karsch[c,d], O. Kaczmarek[d], E. Laermann[d],
R. D. Mawhinney[a], C. Miao[c], P. Petreczky[c,e], C. Schmidt[d], W. Soeldner[†c]

[a] *Physics Department, Columbia University,*
New York, NY 10027, USA
[b] *Department of Physics and Astronomy,*
Stony Brook University, Stony Brook, NY 11790, USA
[c] *Physics Department, Brookhaven National Laboratory,*
Upton, NY 11973, USA
[d] *Fakultät für Physik, Universität Bielefeld,*
D-33615 Bielefeld, Germany
[e] *RIKEN-BNL Research Center,*
Brookhaven National Laboratory, Upton, NY 11973, USA

(Dated: February 3, 2022)

We analyze baryon number, strangeness and electric charge fluctuations as well as their correlations in QCD at high temperature. We present results obtained from lattice calculations performed with an improved staggered fermion action (p4-action) at two values of the lattice cut-off with almost physical up and down quark masses and a physical value for the strange quark mass. We compare these results, with an ideal quark gas at high temperature and a hadron resonance gas model at low temperature. We find that fluctuations and correlations are well described by the former already for temperatures about 1.5 times the transition temperature. At low temperature qualitative features of the lattice results are quite well described by a hadron resonance gas model. Higher order cumulants, which become increasingly sensitive to the light pions, however show deviations from a resonance gas in the vicinity of the transition temperature.

PACS numbers: 11.15.Ha, 11.10.Wx, 12.38Gc, 12.38.Mh

I. INTRODUCTION

Fluctuations of conserved charges, like baryon number, electric charge and strangeness, are generally considered to be sensitive indicators for the structure of (subsets of) a thermal medium produced in heavy ion collisions [1]. In fact, if at non-vanishing baryon number a critical point exists in the QCD phase diagram, this will be signaled by divergent fluctuations of e.g. the baryon number density [2].

Under conditions met in current experiments at RHIC as well as in the upcoming heavy ion experiments at the LHC the net baryon number is small and QCD at vanishing chemical potential provides a good approximation. In this region the transition from the low temperature hadronic to the high temperature plasma regime is continuous and fluctuations are not expected to lead to any singular behavior. Nonetheless, they provide direct insight into the structure of the thermal medium, the relevant degrees of freedom and their correlations. Furthermore, enhanced fluctuations provide hints for nearby singularities in the QCD phase diagram related to the chiral

limit at vanishing net baryon number as well as for a possible critical point at physical values of the quark masses at non-vanishing net baryon number density [3].

Away from criticality, *i.e.* under conditions met at RHIC and LHC, indications for the existence of such critical points can only show up in higher order derivatives of the QCD partition function with respect to temperature or chemical potentials. Through the analysis of fluctuations of conserved charges as well as their higher moments and correlations we thus gain insight into the relevant degrees of freedom of the system under consideration and at the same time gather information on possible nearby singularities in the QCD phase diagram.

From lattice calculations at vanishing chemical potential it is well known that baryon number and strangeness susceptibilities are sensitive indicators for the transition from the low temperature hadronic regime to the high temperature quark gluon plasma. Also in the case of a continuous crossover transition, as is the case for QCD with physical quark masses, the susceptibilities rise rapidly in the transition region [4, 5, 6, 7, 8]. This shows that on the scale of the temperature the (quasi)-particles carrying the quantum numbers under consideration (B, S) are heavy at low and light at high temperature.

In calculations with two light, dynamical quark degrees of freedom (2-flavor QCD) it also has been shown that baryon number and electric charge fluctuations increase and that their fourth moments start to show pro-

[*]current address: Lawrence Livermore National Laboratory Livermore, CA 94550, USA.
[†]current address: Gesellschaft für Schwerionenforschung, Planckstr. 1, D-64291 Darmstadt, Germany.

nounced peaks in the transition region from low to high temperature [7, 9]. In fact, higher order cumulants of e.g. baryon number fluctuations, become increasingly sensitive to the singular behavior in the vicinity of the chiral phase transition at zero mass and vanishing chemical potential. Starting from the 6th order cumulant baryon number fluctuations will diverge in the chiral limit and are expected to reflect critical behavior in accordance with the $O(4)$ symmetric universality of the chiral transition.

It also has been noted that the analysis of correlations between different quantum numbers or flavor channels will provide insight into the quasi-particle structure and the relevant degrees of freedom in QCD at high temperature [10]. In lattice calculations this has been analyzed in quenched [11] and 2-flavor QCD [7, 9, 12]. Recent lattice calculations for the QCD equation of state performed with dynamical light and strange quark degrees of freedom [13, 14] now also allow to perform a systematic analysis of these correlations among different quantum number channels including effects arising from the treatment of strange quarks as dynamical degrees of freedom [8, 15].

We present here results from lattice calculations of baryon number, electric charge and strangeness fluctuations in QCD with dynamical light and strange quark degrees of freedom[1]. The results are based on calculations with an improved staggered fermion action (p4-action) that strongly reduces lattice cut-off effects in bulk thermodynamics at high temperature. The values of the quark masses used in this calculation are almost physical; the strange quark mass, m_s, is fixed to its physical value while the light up and down quark masses are taken to be degenerate and equal to $m_s/10$. This is about twice as large as the average up and down quark masses realized in nature. We obtained results from calculations performed with two different values of the lattice cut-off, corresponding to lattices with temporal extent $N_\tau = 4$ and 6. This allows us to judge the magnitude of systematic effects arising from discretization errors in our improved action calculations. The spatial volume has been chosen to be $V^{1/3}T = 4$, which insures that finite volume effects are small.

II. FLUCTUATIONS AND CORRELATIONS; COMPUTATIONAL SETUP

At vanishing baryon number (B), electric charge (Q) and strangeness (S) fluctuations of these quantities can be obtained by starting from the QCD partition function with non-zero light and strange quark chemical potentials, $\hat{\mu}_{u,d,s} \equiv \mu_{u,d,s}/T$. The quark chemical poten-

tials can be expressed in terms of chemical potentials for baryon number (μ_B), strangeness (μ_S) and electric charge (μ_Q),

$$
\begin{aligned}
\mu_u &= \frac{1}{3}\mu_B + \frac{2}{3}\mu_Q \ , \\
\mu_d &= \frac{1}{3}\mu_B - \frac{1}{3}\mu_Q \ , \\
\mu_s &= \frac{1}{3}\mu_B - \frac{1}{3}\mu_Q - \mu_S \ .
\end{aligned}
\tag{1}
$$

Moments of charge fluctuations, $\delta N_X \equiv N_X - \langle N_X \rangle$, with $X = B$, Q or S and their correlations are then obtained from derivatives of the logarithm of the QCD partition function, $i.e.$ the pressure,

$$
\frac{p}{T^4} \equiv \frac{1}{VT^3} \ln Z(V, T, \mu_B, \mu_S, \mu_Q) \ ,
\tag{2}
$$

evaluated at $\mu_{B,Q,S} = 0$,

$$
\chi_{ijk}^{BQS} = \left. \frac{\partial^{i+j+k} p/T^4}{\partial \hat{\mu}_B^i \partial \hat{\mu}_Q^j \partial \hat{\mu}_S^k} \right|_{\mu=0} ,
\tag{3}
$$

with $\hat{\mu}_X \equiv \mu_X/T$. While the first derivatives, $i.e.$ baryon number, electric charge and strangeness densities, vanish for $\hat{\mu}_{B,Q,S} = 0$, their moments and correlation functions with $i + j + k$ even are non-zero. The basic quantities we will analyze here are the quadratic and quartic charge fluctuations[2],

$$
\begin{aligned}
\chi_2^X &= \frac{1}{VT^3}\langle N_X^2 \rangle \\
\chi_4^X &= \frac{1}{VT^3}\left(\langle N_X^4 \rangle - 3\langle N_X^2 \rangle^2\right) \ ,
\end{aligned}
\tag{4}
$$

and the correlations among two conserved charges,

$$
\chi_{11}^{XY} = \frac{1}{VT^3}\langle N_X N_Y \rangle \ .
\tag{5}
$$

These quantities have been evaluated in the temperature interval $0.8 \lesssim T/T_c \lesssim 2.5$ on lattices of size $16^3 \times 4$ and $24^3 \times 6$, respectively. On the $16^3 \times 4$ lattice we also calculated 6th order expansion coefficients,

$$
\chi_6^X = \frac{1}{VT^3}\left(\langle N_X^6 \rangle - 15\langle N_X^4 \rangle\langle N_X^2 \rangle + 30\langle N_X^2 \rangle^3\right)
\tag{6}
$$

The gauge field configurations, that have been used to evaluate the above observables, had been generated previously in calculations of the QCD equation of state [14] and the transition temperature [16]. In these calculations the strange quark mass has been tuned close to its physical value and the light quark masses have been chosen to be one tenth of the strange quark mass. This corresponds

---

[1] Preliminary results of this calculation had been presented at Lattice 2007 and 2008 [15].

[2] As all expectation values have been evaluated at vanishing chemical potential, we have $\delta N_X \equiv N_X$.

$N_\tau = 4$				$N_\tau = 6$			
T[MeV]	#Conf.	Sep.	#r.v.	T[MeV]	#Conf.	Sep.	#r.v.
176	1013	20	480	174	985	10	400
186	1550	30	480	180	910	10	400
191	1550	30	480	186	1043	10	400
195	1550	30	384	195	924	10	400
202	1550	30	384	201	873	10	350
205	475	60	384	205	717	10	200
219	264	60	384	211	690	10	150
218	950	30	384	224	560	10	150
254	199	60	192	238	670	10	100
305	302	60	96	278	540	10	50
444	618	10	48	363	350	10	50
				416	345	10	50

TABLE I: The data samples analyzed on lattices of temporal extent $N_\tau = 4$ and 6, respectively. The columns give from left to right the temperature values, the number of configurations used in this calculation, the number of trajectories by which these configurations are separated and the number of random vectors used for the evaluation of traces.

to a line of constant physics on which the kaon mass is close to its physical value and the lightest pseudo-scalar mass[3] is about 220 MeV, *i.e.* the light quark masses used in these calculations are about a factor 2 larger than their physical values. Further details on the improved gauge and staggered fermion actions used in these calculations are given in [14, 16]. The number of gauge field configurations analyzed varies from about 300 at high to 1500 at low temperatures. Subsequent configurations are separated by 10 to 60 trajectories. The various operators contributing to χ_{ijk}^{BQS} have been calculated using unbiased random estimators [18]. While at high temperature already 50 random sources per configuration were sufficient to get reliable estimates for these observables, we used up to 480 random sources below the transition temperature. Autocorrelations of the operators contributing to the quadratic and quartic fluctuations turned out to be about 100 trajectories close to T_c and to drop quickly away from it. Errors on these fluctuations have been determined by means of the jack-knife procedure. Some

---

[3] In calculations with staggered fermions flavor symmetry is broken at non-vanishing values of the lattice spacing a. As a consequence only one of the pseudo-scalar mesons has a light mass that is proportional to $\sqrt{m_l}$ and vanishes in the chiral limit at fixed $a > 0$. Full chiral symmetry with the correct Goldstone pion multiplet is recovered only for $a \to 0$. For a study of the remaining flavor symmetry violations with the p4-action in the quenched case see [17]. For dynamical calculations discussed here we have calculated one of the non-Goldstone pion masses at cut-off values corresponding to the transition region of our $N_\tau = 4$ and 6 calculations. This gives 700 MeV and 550 MeV, respectively.

details on our data sample are given in Table I.

In the following we will present our results using a physical temperature scale in MeV. As explained in detail in Ref. [14], this scale has been obtained through detailed studies of the zero temperature static quark potential along the line of constant physics used also for the finite temperature calculations. This yields unambiguously the temperature in units of the lattice scale r_0 that characterizes the shape of the potential at distance r_0, *i.e.* r_0 is defined through the relation $\left(r^2 \mathrm{d}V_{\bar{q}q}(r)/\mathrm{d}r\right)_{r=r_0} = 1.65$. Although r_0 is not directly accessible in experiments, its value is quite well known through comparison with determinations of, e.g. the level splitting in the bottomonium system as well as calculations of light meson decay constants [19, 20]. For the conversion to physical units we have used the value $r_0 = 0.469$ fm [20].

In calculations with the improved staggered action the transition temperature has been determined on lattices with temporal extent $N_\tau = 4$ and 6 for the values of quark masses used here [14, 16]. This gave $T_c = 204(2)$ MeV for $N_\tau = 4$ and 196(3) MeV for $N_\tau = 6$, respectively. The temperature values given in Tables I-III have been obtained from a fit to r_0/a. The fitting function is given in Eq. 22 of Ref. [14]. We therefore do not quote errors on individual temperature values in the table. As discussed in Ref. [14], these errors are generally below 1%.

III. FLUCTUATIONS OF LIGHT AND STRANGE QUARK NUMBERS

Before entering a discussion of fluctuations of B, Q and S it is instructive to look into fluctuations of the partonic degrees of freedom, the light and strange quarks. It has been noticed before that close to the transition temperature fluctuations of the heavier strange quarks are suppressed relative to those of the light u or d quarks [12]. At higher temperatures, however, they approach each other. In these earlier calculations, however, the strange quark sector has not been incorporated as a dynamical degree of freedom in the numerical calculations. Nonetheless, the basic observation also holds true in QCD calculations with dynamical strange quarks.

The difference in the behavior of light and strange quark fluctuations is apparent from Fig. 1, where we show the quadratic fluctuations of light and strange quark numbers (upper figure) and the ratio of these fluctuations (lower figure). The quadratic fluctuations rapidly approach the Stefan-Boltzmann, ideal gas value, $\chi_2^{SB} = 1$, and decrease strongly in the transition region. The calculations on lattices with temporal extent $N_\tau = 4$ and 6 show some cut-off dependence, which is larger for light quarks than for strange quarks. Nonetheless, it is apparent that the approach to the high temperature limit is slower for the heavier strange quarks than for the light up or down quarks. This is highlighted in the lower part of Fig. 1 where we show the ratio of strange to light quark fluctuations. This ratio shows less cut-off depen-

T[MeV]	χ_2^u	χ_2^s	χ_4^u	χ_4^s
176.0	0.1656(28)	0.0922(9)	0.551(38)	0.199(5)
186.4	0.3530(41)	0.2186(20)	1.246(121)	0.561(22)
190.8	0.4298(50)	0.2660(30)	1.662(84)	0.722(25)
195.4	0.5144(74)	0.3190(46)	2.199(127)	0.968(39)
202.4	0.7095(58)	0.4464(38)	2.315(122)	1.189(48)
204.8	0.7689(66)	0.4918(49)	1.762(154)	1.117(65)
209.6	0.9452(52)	0.6577(54)	1.140(98)	1.104(58)
218.2	1.0040(27)	0.7371(25)	0.857(29)	1.013(25)
253.7	1.0556(28)	0.9078(25)	0.594(19)	0.754(16)
305.2	1.0543(21)	0.9851(18)	0.543(12)	0.631(13)
444.4	1.0158(5)	0.9913(5)	0.515(7)	0.536(7)

T[MeV]	χ_2^u	χ_2^s	χ_4^u	χ_4^s
173.8	0.2077(77)	0.1167(35)	0.803(210)	0.244(18)
179.6	0.2769(85)	0.1643(32)	0.915(225)	0.310(36)
185.6	0.3950(81)	0.2341(45)	1.348(122)	0.563(40)
195.0	0.6011(116)	0.3743(93)	1.786(196)	0.963(112)
201.3	0.7556(80)	0.5027(58)	1.001(94)	0.843(49)
204.6	0.8093(86)	0.5630(53)	0.935(80)	0.816(48)
211.1	0.8714(65)	0.6483(49)	0.809(87)	0.879(66)
224.3	0.9313(61)	0.7219(62)	0.667(75)	0.900(63)
237.7	0.9695(33)	0.8319(39)	0.571(56)	0.731(43)
278.4	0.9975(48)	0.9439(21)	0.576(36)	0.591(32)
362.9	1.0181(35)	1.0039(21)	0.543(22)	0.549(11)
415.8	1.0163(18)	1.0044(30)	0.541(12)	0.563(25)

TABLE II: The data on quadratic and quartic fluctuations of light (u, d) and strange (s) quarks obtained from calculations on $16^3 \times 4$ (upper table) and $24^3 \times 6$ (lower table) lattices, respectively.

FIG. 1: The quadratic fluctuations of light and strange quark number versus temperature (upper figure) and the ratio of s and u quark fluctuations on lattices of size $16^3 \times 4$ and $24^3 \times 6$, respectively. The solid lines show results for an ideal Fermi gas with mass $m = 100$ MeV and 200 MeV, respectively (top to bottom). In the lower figure we also show partially quenched results obtained with unimproved staggered fermions on $16^3 \times 4$ lattices [12]. These results have been given in Ref. [12] as function of T/T_c. This scale is shown on the upper x-axis in the lower part of the figure. We have used the mean value of the transition temperatures on the $N_\tau = 4$ and 6 lattices, i.e. $T_0 = 200$ MeV, to compare with calculations performed with the p4-action.

dence than χ_2^u and χ_2^s separately. In fact, the difference between the $N_\tau = 4$ and 6 results for χ_2^s/χ_2^u is well understood in terms of the small shift (cut-off dependence) of the transition temperature determined for these two different lattice sizes.

We find that χ_2^s/χ_2^u is about 0.6 at T_c and approaches unity at about $1.7T_c$. In both figures we show a band indicating the result for fluctuations in a non-interacting, massive Fermi gas. As can be seen this can explain the smaller fluctuations of strange quarks relative to light quarks only at temperatures larger than about 300 MeV, i.e. for $T \gtrsim 1.5\, T_c$. In quenched QCD and QCD with n_f massless quark flavors the approach to the high temperature limit has also been analyzed within HTL-resummed perturbation theory [21] as well as in a straightforward perturbative calculation performed up to $\mathcal{O}(g^6 \ln g)$ [22]. In both cases the results resemble closely properties of a Fermi gas with a temperature dependent mass term. Both approaches, however, use additional phenomenological input to either re-sum next-to-leading order corrections to the HTL mass or fix the unknown scale for the $\mathcal{O}(g^6 \ln g)$ correction. The lattice results presented in Fig. 1 overshoot the HTL result by about 5%. This is of
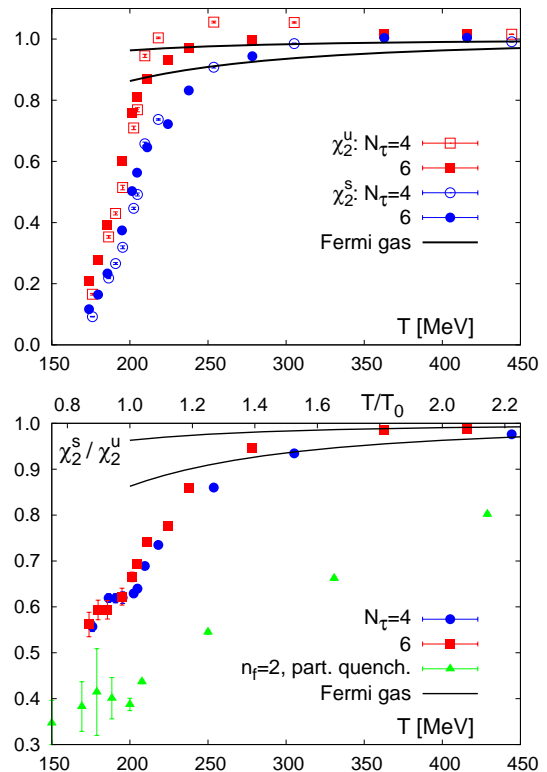
similar magnitude as the cut-off dependence seen in the current lattice results when comparing the $N_\tau = 4$ and 6 data in the temperature interval $1.5 \lesssim T/T_c \lesssim 2$. In view of the large change between the leading and the next to leading order HTL calculations as well as the systematics of the cut-off dependence seen in the lattice results, this seems to be a reasonably good agreement.

We note that the results shown in Fig. 1 are in agreement with calculations performed with another improved staggered fermion action [6, 8], the asqtad action. The results obtained with improved (p4 and asqtad) actions are, however, in contrast to calculations performed with the standard staggered action in quenched [11] and 2-flavor [12] QCD. These calculations led to significantly larger values for χ_2, which is understood in terms of the large cut-off effects in the standard discretization scheme (see appendix). In the absence of results on larger lat-

tices, which would have allowed for a continuum extrapolation, the numerical results obtained within the standard discretization scheme [11, 12] have been normalized to the corresponding ideal gas value evaluated also on lattices with finite temporal extent. It is well known that at temperatures a few times the transition temperature this procedure, which is correct in the limit of infinite temperature, over-estimates the actual cut-off distortion of numerical results. The normalized values thus end up to be substantially smaller than the results obtained with improved staggered fermion actions for which an ad-hoc normalization has not been performed. We discuss cut-off effects and their quark mass dependence for the standard and p4-action in somewhat more detail in the appendix.

The situation is different for the ratio χ_2^s/χ_2^u shown in the lower part of Fig. 1. Here unknown normalization factors drop out. Nonetheless, also in this case results obtained in calculations with improved actions are significantly larger than those obtained with a standard action. This difference may be due to the fact that in Ref. [12] the strange quark sector has only been treated in the quenched approximation.

IV. FLUCTUATION OF CONSERVED CHARGES

In Fig. 2 we show results for quadratic (χ_2^X) and quartic (χ_4^X) fluctuations with $X = B$, Q and S. As can be seen, in all cases the quadratic fluctuations rise rapidly in the transition region where the quartic fluctuations show a maximum. This maximum is most pronounced for the baryon number fluctuations but is still visible also in fluctuations of the strangeness number.

We note that results obtained on lattices with temporal extent $N_\tau = 6$ are in good agreement with those obtained on the coarser $N_\tau = 4$ lattice. The slight shift towards smaller temperatures, visible for the $N_\tau = 6$ data relative to the $N_\tau = 4$ data, is consistent with findings for the equation of state, e.g. the trace anomaly $(\epsilon - 3p)/T^4$, and also reflects the shift in the transition temperature observed when comparing the location of cusp in the chiral susceptibility [16]. The generic form of this temperature dependence, a smooth crossover for quadratic fluctuations and a peak in quartic fluctuations, is in fact expected to occur in the vicinity of the chiral phase transition of QCD. At vanishing chemical potential and for vanishing quark mass the singular behavior of fluctuation observables like, e.g. the baryon number cumulants, is expected to be controlled by the singular part of the free energy that has the same universal structure as that of a three dimensional $O(4)$ spin model[4].

---

[4] As chiral symmetry is explicitly broken in numerical calculations with staggered fermions, the relevant symmetry group is, in fact,

T[MeV]	χ_2^B	χ_2^Q	χ_4^B	χ_4^Q
176.0	0.0301(9)	0.1229(8)	0.028(12)	0.189(5)
186.4	0.0831(25)	0.2433(17)	0.083(16)	0.415(17)
190.8	0.1061(19)	0.2903(29)	0.137(18)	0.521(26)
195.4	0.1328(32)	0.3412(43)	0.193(15)	0.682(30)
202.4	0.1931(17)	0.4601(35)	0.193(36)	0.744(35)
204.8	0.2133(33)	0.4961(39)	0.111(25)	0.599(41)
209.6	0.2694(23)	0.6154(38)	0.072(14)	0.365(43)
218.2	0.2978(5)	0.6480(18)	0.060(5)	0.259(11)
253.7	0.3313(18)	0.6918(12)	0.034(6)	0.159(6)
305.2	0.3398(10)	0.6992(11)	0.023(5)	0.143(3)
444.4	0.3343(3)	0.6760(5)	0.019(2)	0.127(1)
T[MeV]	χ_2^B	χ_2^Q	χ_4^B	χ_4^Q
173.8	0.0395(36)	0.1517(30)	0.094(56)	0.215(10)
179.6	0.0581(48)	0.1980(34)	0.101(54)	0.260(36)
185.6	0.0928(30)	0.2700(47)	0.102(32)	0.435(34)
195.0	0.1600(37)	0.3930(78)	0.142(30)	0.577(69)
201.3	0.2088(31)	0.4928(46)	0.047(18)	0.346(29)
204.6	0.2299(41)	0.5266(38)	0.091(15)	0.270(20)
211.1	0.2528(28)	0.5723(32)	0.067(22)	0.237(18)
224.3	0.2794(21)	0.6058(37)	0.036(17)	0.218(19)
237.7	0.3000(20)	0.6388(15)	0.043(23)	0.156(7)
278.4	0.3232(22)	0.6637(16)	0.029(6)	0.139(7)
362.9	0.3354(11)	0.6798(17)	0.021(7)	0.135(5)
415.8	0.3362(10)	0.6777(12)	0.023(4)	0.131(2)

TABLE III: The data on quadratic and quartic fluctuations obtained from calculations on $16^3 \times 4$ (upper table) and $24^3 \times 6$ (lower table) lattices, respectively.

This singular part of the free energy, f_s, is controlled by a reduced 'temperature' t that is a function of temperature as well as the quark chemical potentials μ_X [23, 24]. The latter add in even combinations to the reduced temperature in order to respect charge symmetry at $\mu_X = 0$. Baryon number cumulants are thus expected to scale like,

$$\chi_{2n}^B \sim \left| \frac{T - T_c}{T_c} \right|^{2-n-\alpha} \qquad (7)$$

with $\alpha \simeq -0.25$ $[-0.015]$ [25] denoting the critical exponent characterizing the non-analytic structure of the specific heat in 3-d, $O(4)$ $[O(2)]$ symmetric spin models. Starting at 6th order the baryon number cumulant thus will diverge at T_c in the chiral limit. It has been argued in [7] that this singularity will also show up in cumulants of the electric charge.

On lattices with temporal extent $N_\tau = 4$ and 6 and for the values of quark masses used here the transition temperature is close to 200 MeV. From Fig. 2 we thus
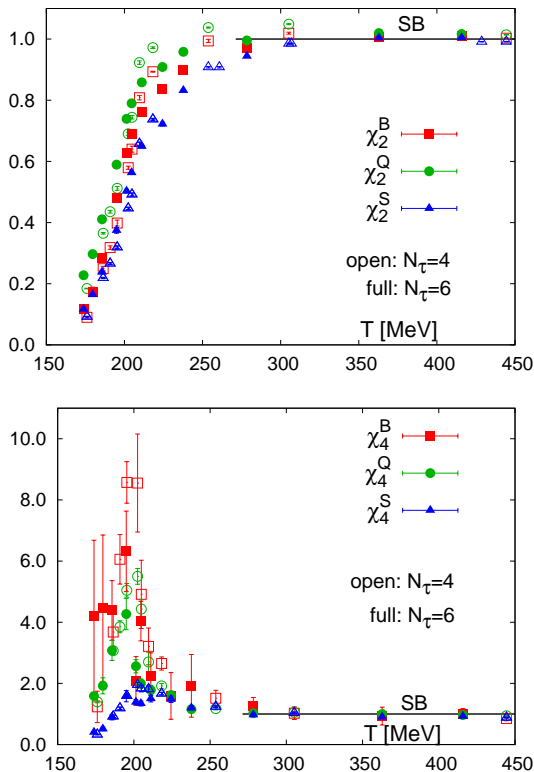
---

expected to be $O(2)$.

FIG. 2: Quadratic and quartic fluctuations of baryon number, electric charge and strangeness. All quantities have been normalized to the corresponding free quark gas values, $\chi_n^{X,SB}$ given in Table IV.

X	B	Q	S
$\chi_2^{X,SB}$	1/3	2/3	1
$\chi_4^{X,SB}$	$2/9\pi^2$	$4/3\pi^2$	$6/\pi^2$

TABLE IV: Ideal gas values for quadratic (χ_2) and quartic (χ_4) fluctuations of baryon number (B), electric charge (Q) and strangeness (S).

conclude that at temperatures of about $1.5T_c$ and larger quadratic and quartic cumulants of the fluctuations of B, Q and S are close to those of an ideal, massless quark gas, for which the pressure is given by

$$\frac{p^{SB}}{T^4} = \sum_{f=u,d,s} \left[\frac{7\pi^2}{60} + \frac{1}{2}\left(\frac{\mu_f}{T}\right)^2 + \frac{1}{4\pi^2}\left(\frac{\mu_f}{T}\right)^4 \right] . (8)$$

Using the relations given in Eq. 1 one easily derives the corresponding ideal gas values for quadratic and quartic fluctuations of conserved charges. These are summarized in Table IV.

The upper part of Fig. 2 shows that over a wide temperature range quadratic fluctuations of strangeness are suppressed relative to those of baryon number and charge, which receive contributions also from fluctua-
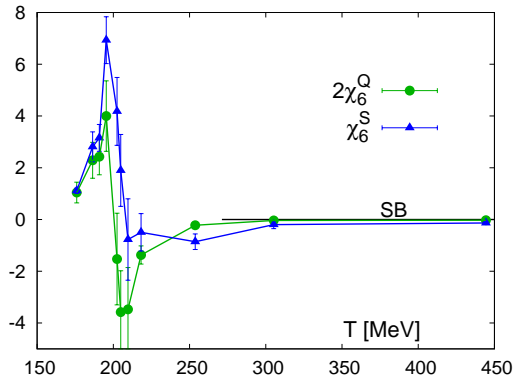

FIG. 3: The 6th order cumulant of electric charge and strangeness fluctuations evaluated on lattices of size $16^3 \times 4$.

tions of the light u and d quarks. Only for temperatures $T \gtrsim 1.7T_c$ do the fluctuations of all three charges agree. This resembles the pattern of the relative strength of light and strange quark fluctuations seen in Fig. 1.

On the coarser $N_\tau = 4$ lattices we also have calculated the 6th order cumulants, χ_6^X, which vanish in the infinite temperature, ideal gas limit as well as in leading order perturbation theory [21]. For strangeness and charge fluctuations we show results in Fig. 3. Note that these 6th order cumulants change sign at $T \simeq T_c$. Below T_c they rise rapidly and reach a maximum at $T \simeq 0.95T_c$; they approach zero from below and almost vanish for $T \gtrsim 1.5T_c$.

V. RATIOS OF CUMULANTS

At low temperatures hadrons are the relevant degrees of freedom. The hadron resonance gas (HRG) model has been shown to provide a good description of thermal conditions at freeze-out [26, 27]. Also fluctuations of the thermal medium have been successfully described in the framework of a HRG model [28]. Nonetheless, in a HRG model cumulants are monotonically rising functions of the temperature, while the 6th order cumulants change sign at T_c. This indicates that a straightforward HRG model has to break down in the vicinity of the transition temperature.

The partition function of the hadron resonance gas can be split into mesonic and baryonic contributions,

$$p^{HRG}/T^4 = \frac{1}{VT^3} \sum_{i \in mesons} \ln \mathcal{Z}_{m_i}^M(T, V, \mu_B, \mu_Q, \mu_S)$$
$$+ \frac{1}{VT^3} \sum_{i \in baryons} \ln \mathcal{Z}_{m_i}^B(T, V, \mu_B, \mu_Q, \mu_S) , (9)$$

where

$$\ln \mathcal{Z}_{m_i}^{M/B} = \mp \frac{V d_i}{2\pi^2} \int_0^\infty dk k^2 \ln(1 \mp z_i e^{-\varepsilon_i/T}) , \quad (10)$$
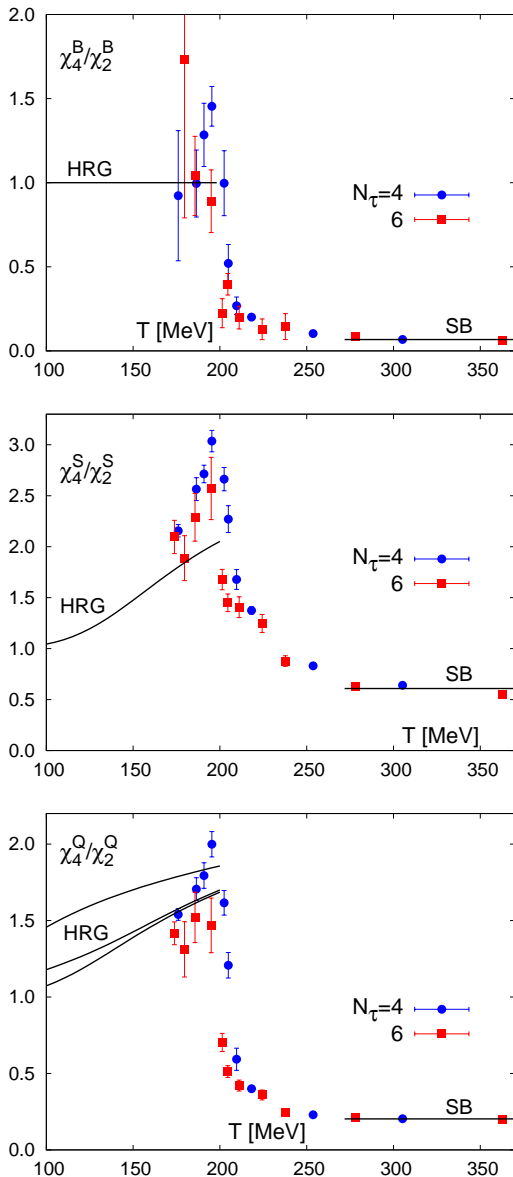
FIG. 4: The ratio of fourth and second order cumulants of baryon number (top), strangeness (middle) and electric charge (bottom) fluctuations. In the latter case we show curves for a HRG model calculated with physical pion masses (upper curve), pions of mass 220 MeV (middle) and infinitely heavy pions (lower curve).

with energies $\varepsilon_i = \sqrt{k^2 + m_i^2}$, degeneracy factors d_i and fugacities

$$z_i = \exp\left((B_i\mu_B + Q_i\mu_Q + S_i\mu_S)/T\right) . \quad (11)$$

The HRG model has been compared to lattice results previously [28]. In these earlier comparisons with lattice calculations, which had to be performed with rather large quark masses and without dynamical strange quarks the masses contributing to the HRG model were adjusted and strange contributions were suppressed. Here we no

longer follow this strategy but compare directly the lattice results with an HRG model that is based on the experimentally observed spectrum. We use the same HRG model as it also is used in heavy ion phenomenology and the analysis of freeze-out conditions [26, 27]. This ansatz for the HRG includes all meson and baryon masses from the particle data book with masses $m_i \leq 2.5$ GeV that are characterized at least as '4 star states'.

Also on the lattice with temporal extent $N_\tau = 6$ calculations at low temperature are still performed on quite coarse lattices. We thus cannot expect to reproduce details of the hadron spectrum well under these conditions. Nevertheless, we feel that it is now most appropriate to compare lattice results directly with the unmodified continuum version of the HRG model that is commonly used in the phenomenological treatment of QCD thermodynamics. By improving lattice calculations systematically one will then be able to judge to what extent the HRG model does describe the thermodynamics of QCD in the hadronic phase. In fact, the current calculations of the QCD equation of state, e.g. the pressure and trace anomaly, $(\epsilon - 3p)/T^4$, show deviations from the HRG at temperatures below the transition region. This is still the case in calculations on lattices with temporal extent $N_\tau = 8$, i.e. closer to the continuum limit [29, 30]. We thus concentrate here on observables which are less sensitive to details of the hadron mass spectrum and emphasize the charges of the relevant degrees of freedom contributing to the fluctuations. These are in general ratios of cumulants of N_B, N_Q, and N_S. In fact, in the framework of a HRG model it is easy to convince oneself that the ratio of fourth and second order cumulants of baryon number fluctuations is completely independent of the actual value of hadron masses; $(\chi_4^B/\chi_2^B)_{HRG} = 1$ if all hadrons are heavy on the scale of the temperature. In that case the fugacity expansion of Eq. 10,

$$\ln Z_m^B = \frac{VT^3}{\pi^2}\left(\frac{m}{T}\right)^2 \sum_{\ell=1}^{\infty}(-1)^{\ell+1}\,\ell^{-2}\,K_2(\ell m/T)$$
$$\times \cosh(\ell\mu_B/T) \quad , \quad (12)$$

is well approximated by its leading order term, i.e. the Boltzmann approximation. In this case the baryonic contribution to the pressure of a HRG is proportional to $\cosh(\mu_B/T)$ and the ratio χ_4^B/χ_2^B thus becomes independent of the hadron mass spectrum. This is reasonably well reproduced by the lattice results shown in Fig. 4(top). Note, however, that in the chiral limit it is expected that the cusp in χ_4^B (Fig. 2) is expected to become more pronounced and thus more prominent also in the ratio χ_4^B/χ_2^B. How strong this effect will be requires more detailed studies and also a better control over the continuum limit. Model calculations yield quite a different strength for the peak in χ_4^B/χ_2^B [31].

Even within the Boltzmann approximation the structure of a HRG is, however, more complicated in the strange and/or electrically charged sectors. In these cases multiply strange hadrons or hadrons with charge $Q = 2$

contribute to the HRG. This enhances quartic fluctuations relative to quadratic ones and leads to a deviation of cumulant ratios from unity. This qualitative feature is indeed seen in the results obtained for χ_4^S/χ_2^S and χ_4^Q/χ_2^Q shown in Fig. 4, respectively.

We note that the lightest hadrons, the pions, only contribute to cumulants of electric charge fluctuations. For these light states the Boltzmann approximation is not sufficient at temperatures close to T_c. We thus have used the complete bosonic fugacity sum in the pion sector. These light hadronic states are also not well taken into account in current lattice calculations which still are being performed with light quark masses that are about a factor two larger than the physical up and down quark masses. Moreover, the pion spectrum is distorted in calculations with staggered fermions due to cut-off effects that explicitly break flavor symmetry at non-vanishing lattice spacing (see footnote 3). In the case of electric charge fluctuations we therefore have analyzed in more detail the contribution of pions to the fluctuations in a HRG. In Fig. 4(bottom) we show results for HRG model calculations with physical pion masses, with a pion mass of 220 MeV, which corresponds to the lightest pseudo-scalar state formed with the quark mass values currently used in our calculations, and without the pion sector, $i.e.$ for infinitely heavy pions. Although the largest part of the electric charge fluctuations arises from heavier hadrons, the ratio of cumulants is sensitive to the pion sector. Already pion masses that are 50% larger than the physical value drastically reduce the contribution of the pion sector. This effect is even more significant in higher order cumulants. In the 6th order cumulant half of the fluctuations can be attributed to the light pion sector. This is obvious from Fig. 5 where we show the ratio of 6th and 2nd order cumulants for electric charge fluctuations. In a HRG model the ratio of cumulants calculated without the light pion sector is a factor two smaller than that calculated with the physical pions included. In the low temperature regime the lattice calculations are consistent with the former. We thus conclude that lighter quark masses and calculations closer to the continuum limit are needed to correctly represent in lattice calculations higher order cumulants that are sensitive to the light hadron sector. Irrespective of this we find, however, that the occurrence of maxima in χ_6^X close but below T_c signal the breakdown of the HRG model close to T_c. The ratio χ_6^Q/χ_2^Q starts dropping below T_c and is consistent with zero at T_c.

A similar behavior is found for higher order cumulants of strangeness fluctuations. We find that for both values of the lattice cut-off the ratio χ_4^S/χ_2^S overshoots the HRG values in the transition region and this also holds true for the ratio χ_6^S/χ_2^S evaluated on the coarse $16^3 \times 4$ lattices. Of course, this requires confirmation through calculations with lighter quark masses on lattices closer to the continuum limit. It may suggest that the contribution of even heavier, experimentally not well-established multiple strange hadrons, which are not included in the
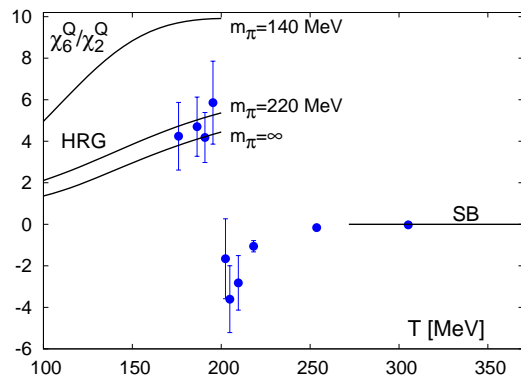

FIG. 5: The ratio of 6th and 2nd order cumulants of electric charge fluctuations evaluated on lattices of size $16^3 \times 4$.

current version of the HRG model, is of importance in the transition region. In general we find, however, that the HRG model gives a fairly good description of cumulants of the fluctuations of conserved charges up to temperatures close to the transition temperature.

VI. CORRELATIONS AMONG CONSERVED CHARGES

The analysis of cumulant ratios presented in the previous section suggests that for temperatures above $1.5T_c$ fluctuations of baryon number, strangeness and electric charge agree well with the corresponding fluctuations in a non-interacting gas of light and strange quarks. In order to further test whether the relevant quasi-particle degrees of freedom indeed can be assigned to quarks, the analysis of correlations between different charges is quite instructive [10, 12]. Results for correlations between N_B, N_S and N_Q are shown in Figs. 6 and 7. For completeness we also include the HRG-prediction. We note that the model is not expected and, in fact, does not capture the fluctuations and correlations in the transition region correctly. However, as shown in Figs. 6 and 7 as well as in Fig. 4 it reproduces qualitatively the features of fluctuations and correlations. In particular, the drop and rise seen in our numerical results for BQ and BS correlations, respectively, is seen also in the HRG model calculations. To put these observations on a more quantitative basis will require further calculations at lower temperatures.

In Fig. 6 the correlation functions in the numerator project only on the charged baryon sector of the spectrum. The ratio χ_{11}^{BQ}/χ_2^B therefore approaches[5] $1/2$ in the low temperature limit as the numerator receives contributions from protons and anti-protons only, while the

---

[5] We ignore here small mass differences of charged and neutral hadrons.

T[MeV]	χ_{11}^{BQ}	χ_{11}^{BS}	χ_{11}^{QS}
176.0	0.00630(35)	-0.0175(9)	0.0374(2)
186.4	0.01332(40)	-0.0564(14)	0.0811(5)
190.8	0.01670(26)	-0.0727(13)	0.0966(9)
195.4	0.02023(43)	-0.0924(19)	0.1133(14)
202.4	0.02811(32)	-0.1369(14)	0.1548(13)
204.8	0.02959(41)	-0.1544(20)	0.1687(15)
209.6	0.03024(58)	-0.2089(19)	0.2244(19)
218.2	0.02912(17)	-0.2395(8)	0.2488(9)
253.7	0.01625(12)	-0.2988(16)	0.3045(6)
305.2	0.00765(6)	-0.3245(11)	0.3303(5)
444.4	0.00272(1)	-0.3289(4)	0.3312(3)

T[MeV]	χ_{11}^{BQ}	χ_{11}^{BS}	χ_{11}^{QS}
173.8	0.00830(88)	-0.0228(23)	0.0469(8)
179.6	0.01040(120)	-0.0373(26)	0.0635(14)
185.6	0.01611(74)	-0.0606(18)	0.0868(18)
195.0	0.02406(49)	-0.1119(33)	0.1312(31)
201.3	0.02697(72)	-0.1549(24)	0.1739(18)
204.6	0.02641(72)	-0.1771(31)	0.1930(13)
211.1	0.02312(67)	-0.2066(25)	0.2208(16)
224.3	0.02309(90)	-0.2332(25)	0.2444(20)
237.7	0.01529(66)	-0.2695(23)	0.2812(10)
278.4	0.00529(77)	-0.3126(10)	0.3157(8)
362.9	0.00145(63)	-0.3325(8)	0.3357(10)
415.8	0.00122(34)	-0.3338(13)	0.3353(12)

TABLE V: The data on correlations between different quantum number fluctuations obtained from calculations on lattices with temporal extent $N_\tau = 4$ (upper table) and 6 (lower table), respectively.

FIG. 6: Correlations of electric charge and strangeness with baryon number normalized to quadratic fluctuations of baryon number.

denominator also receives contributions from the neutrons. The ratio χ_{11}^{BS}/χ_2^B, however, will approach zero in the low temperature limit as the lightest baryons carry no strangeness!

In Fig. 7 we show the correlation among Q and S normalized to the quadratic fluctuations of electric charge. A similar ratio, where strangeness fluctuations have been used to normalize the Q-S correlations, has been discussed in [10] and has also been calculated in 2-flavor QCD with a quenched strange quark sector [12]. We prefer the above normalization, as it emphasizes the non trivial correlations between Q and S that persist in the high temperature phase of QCD. Unlike χ_2^S the charge fluctuations χ_2^Q approach the ideal gas value rapidly above T_c (see Fig. 2). The deviations from ideal gas behavior seen in Fig. 7 thus are mainly due to the deviations of χ_{11}^{QS} from ideal gas behavior. This is shown in the lower part of Fig. 7. Apparently, the temperature dependence of χ_{11}^{QS} is very similar to that of χ_2^S.
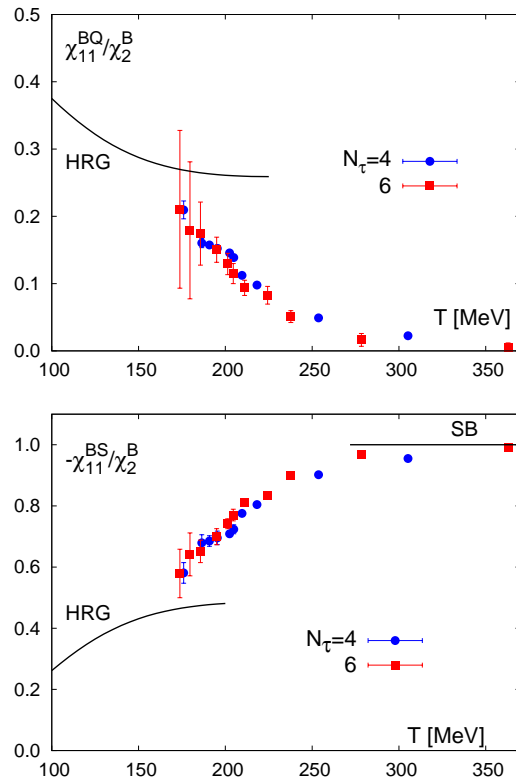
VII.   CONCLUSIONS

We have analyzed the fluctuations of baryon number, electric charge and strangeness in finite temperature QCD at vanishing chemical potential. A comparison of calculations performed with $\mathcal{O}(a^2)$ improved staggered fermions for two different values of the lattice cut-off shows that these effects are generally small; cut-off effects as well as the dependence of observables on the light quark masses become, however, more severe for higher order cumulants.

We find fluctuations and correlations of conserved charges are well described by an ideal, massless quark gas already for temperatures of about $(1.5 - 1.7)$ times the transition temperature. Deviations from ideal gas behavior seem to be mainly induced by the strange quark sector for which the quadratic quark number fluctuations approach the ideal gas limit more slowly. This cannot only be explained by the quark mass dependence of an ideal gas but seems to reflect a significant quark mass dependence of the interaction at high temperature.

At low temperature we find that fluctuations and correlations of conserved charges are reasonably well described by a hadron resonance gas up to temperatures close to the transition temperature. Higher order cumulants, however, signal that the resonance gas prescription
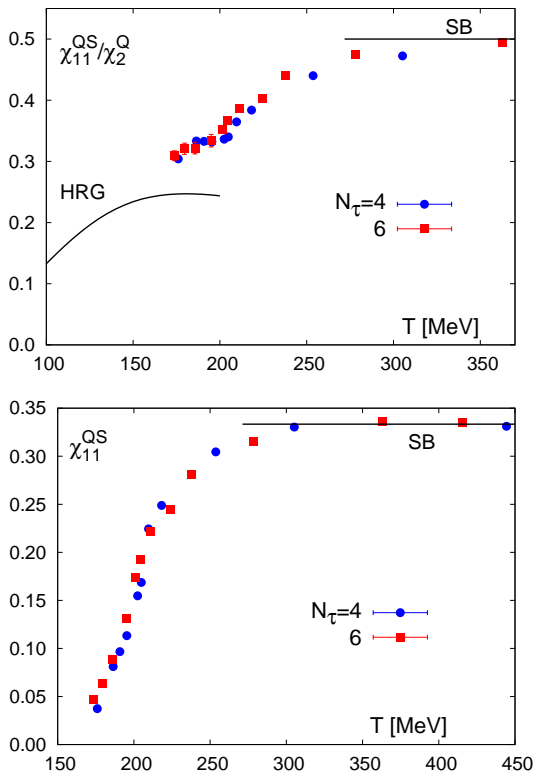
FIG. 7: Correlations of electric charge and strangeness (lower part) and the same quantity normalized to quadratic fluctuations of electric charge (upper part).

has to break down at temperature values close but below T_c.

The current analysis has been performed with light quarks that are one tenth of the strange quark mass. We have shown, that higher order cumulant ratios like, for instance χ_6^Q/χ_2^Q, become quite sensitive to the pseudo-scalar Goldstone mass. In numerical calculations with staggered fermions this also means that results become sensitive to a correct representation of the entire Goldstone multiplet. Calculations with smaller quark masses closer to the continuum limit will thus be needed in the future to correctly resolve these higher order cumulants, which will give deeper insight into the range of applicability of the resonance gas model at low temperature and the non-perturbative features of the QGP above but close to T_c.

APPENDIX: QUARK MASS DEPENDENCE OF CUT-OFF EFFECTS

Cut-off effects arising from the introduction of a finite lattice spacing and, in particular, their dependence on the discretization scheme have been extensively discussed in the ideal gas limit. However, standard as well as $\mathcal{O}(a^2)$ improved staggered fermion formulations have usually been analyzed in the massless limit, which is appropriate for the light quark sector of QCD. For the strange quark sector non-zero mass effects may play a role, in particular close to the QCD transition temperature which is only about twice as large as the strange quark mass. We present here an analysis of the quark mass dependence of cut-off effects in the ideal gas limit.

The quark number susceptibilities are obtained as the second derivative of the pressure, p/T^4, with respect to the chemical potential normalized to the temperature, μ/T. An analysis of the cut-off and quark mass dependence of $\chi_2^{u,s}$ thus can follow closely the corresponding analysis performed for the pressure[6] in the massless limit [32]. On a lattice of size $N_\sigma^3 N_\tau$ this is given by

$$\frac{p}{T^4} = 2 \left(\frac{N_\tau}{N_\sigma} \right)^3 \sum_{\mathbf{p},p_4} \ln(D^2 + m^2), \qquad (A.1)$$

with, $D^2 = \sum_{\mu=1}^4 D_\mu^2$ where

$$D_1 = c_{10} \sin(p_1) + c_{30} \sin(3p_1) + 2c_{12} \sin(p_1) \times$$
$$[\cos(2p_2) + \cos(2p_3) + \cos(2p_4)] \qquad (A.2)$$

and D_2, D_3 and D_4 are obtained by cyclic permutation of the p_is. For the standard (naive) discretization scheme, one has $c_{10} = 1$, $c_{30} = c_{12} = 0$; the discretization scheme used in the p4-action corresponds to $c_{10} = 3/4$, $c_{30} = 0$, $c_{12} = 1/24$ and for the Naik action it is $c_{10} = 9/8$ and $c_{30} = -1/24$ and $c_{12} = 0$.

We evaluate here quark number susceptibilities as a function of quark mass on lattices with finite temporal extent N_τ and infinite spatial volume for the standard (naive) staggered fermion discretization and the improved (p4) discretization scheme. For vanishing quark mass results on the cut-off dependence of quark number

---

[6] Note that at vanishing chemical potential the pressure is simply related to the free energy density, $p = -f$.
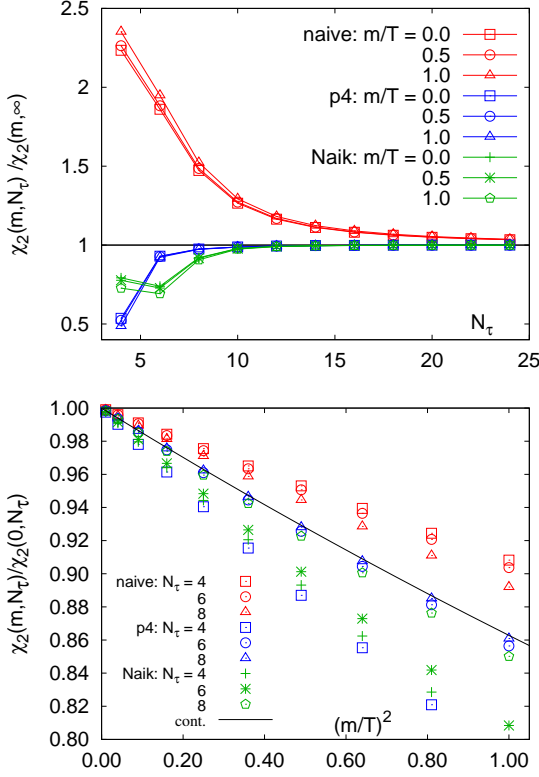
FIG. 8: Cut-off dependence of quark number fluctuations in the infinite temperature, ideal gas limit. Shown are results for staggered fermions in the standard (naive), p4 and Naik discretization scheme.

susceptibilities in the ideal gas limit have also been presented in Ref. [33, 34]. There also some results for χ_4 and χ_6 can be found.

Starting with the expressions for p/T^4 at non-zero chemical potential ($p_4 \to p_4 - i\mu$) and taking two derivatives with respect to μ/T one finds in the standard scheme for $\mu \equiv 0$,

$$\chi_2(m, N_\tau) = 2\left(\frac{N_\tau}{N_\sigma}\right)^3 \sum_{\mathbf{p}, p_4} (A - B + AB),$$

$$A = \frac{2\sin^2(p_4)}{m^2 + \sum_{i=1}^4 \sin^2(p_i)}, \qquad \text{(A.3)}$$

$$B = \frac{2\cos^2(p_4)}{m^2 + \sum_{i=1}^4 \sin^2(p_i)}.$$

the corresponding expressions for the p4 and Naik actions are somewhat more complicated but can be derived straightforwardly.

In the continuum limit the quark number susceptibility is given by,

$$\chi_2(m/T, \infty) = \frac{6}{T^3\pi^2} \int_0^\infty dk \frac{k^2 \, e^{-E/T}}{\left(1 + e^{-E/T}\right)^2} , \qquad \text{(A.4)}$$

with $E^2 = k^2 + m^2$. We note that for small values of the quark mass χ_2 is quadratic in the mass,

$$\chi_2(m/T, \infty) = 1 - \frac{3}{2\pi^2}\left(\frac{m}{T}\right)^2 + \mathcal{O}((m/T)^4) . \qquad \text{(A.5)}$$

We have evaluated $\chi_2(m, N_\tau)$ for various values of N_τ and fixed quark mass as well as for fixed N_τ varying the quark mass. The results for the naive and p4 actions are shown in Fig. 8

As expected, the cut-off dependence of χ_2 at non-zero values of the quark mass closely follow the pattern known from the analysis of the pressure at finite N_τ and $m/T = 0$. While the standard discretization scheme shows large deviations from the continuum result even for $N_\tau \sim 10$, the results for the p4 action come close to the continuum result already for $N_\tau = 6$. This also is true for the ratio $\chi_2(m, N_\tau)/\chi_2(0, N_\tau)$. Although in this ratio a large part of the cut-off dependence cancels, the quark mass dependent corrections remain.

We note, that for finite N_τ the quark mass dependence of $\chi_2(m, N_\tau)/\chi_2(0, N_\tau)$ in the naive discretization scheme is weaker than in the continuum limit. This is qualitatively different from the differences seen in the lower part of Fig. 1 between the standard and improved discretization schemes.

[1] for a recent review see: V. Koch, *Hadronic Fluctuations and Correlations*, arXiv:0810.2520.

[2] M. A. Stephanov, K. Rajagopal and E. V. Shuryak, Phys. Rev. Lett. **81**, 4816 (1998).

[3] for a review see: M. Stephanov, *The phase diagram of QCD and the critical point*, Acta Phys. Polon. B **35**, 2939 (2004).

[4] S. A. Gottlieb *et al.*, Phys. Rev. Lett. **59**, 2247 (1987).

[5] R. V. Gavai, S. Gupta and P. Majumdar, Phys. Rev. D **65**, 054506 (2002).

[6] C. Bernard *et al.* [MILC Collaboration], Phys. Rev. D **71**, 034504 (2005).

[7] C. R. Allton *et al.*, Phys. Rev. D **71**, 054508 (2005).

[8] C. Bernard *et al.*, Phys. Rev. D **77**, 014503 (2008).

[9] S. Ejiri, F. Karsch and K. Redlich, Phys. Lett. B **633**, 275 (2006).

[10] S. Jeon and V. Koch, Phys. Rev. Lett. **85**, 2076 (2000); V. Koch, A. Majumder and J. Randrup, Phys. Rev. Lett. **95**, 182301 (2005)

[11] R. V. Gavai and S. Gupta, Phys. Rev. D **64**, 074506 (2001).

[12] R. V. Gavai and S. Gupta, Phys. Rev. D **73**, 014004 (2006).

[13] C. Bernard *et al.*, Phys. Rev. D **75**, 094505 (2007).

[14] M. Cheng *et al.*, Phys. Rev. D **77**, 014511 (2008).

[15] C. Miao and C. Schmidt, PoS **LAT2007**, 175 (2007) and PoS **LAT2008**, 172 (2008).

[16] M. Cheng *et al.*, Phys. Rev. D **74**, 054507 (2006).

[17] M. Cheng *et al.*, Eur. Phys. J. C 51, 857 (2008).

[18] C. R. Allton *et al.*, Phys. Rev. D **66**, 074507 (2002)

[19] C. T. H. Davies *et al.* [HPQCD Collaboration and UKQCD Collaboration and MILC Collaboration], Phys. Rev. Lett. **92**, 022001 (2004).

[20] A. Gray *et al.*, Phys. Rev. **D72**, 094507 (2005).

[21] J.-P. Blaizot, E. Iancu and A. Rebhan, Phys. Lett. B **523**, 143 (2001).

[22] A. Vuorinen, Phys. Rev. D **67**, 074032 (2003)

[23] Y. Hatta and T. Ikeda, *Phys. Rev. D* **67**, 014028 (2003).

[24] F. Karsch, PoS **CPOD07**, 026 (2007).

[25] A. Pelissetto and E. Vicari, Phys. Rept. **368**, 549 (2002)

[26] J. Cleymans and K. Redlich, Phys. Rev. C **60**, 054908 (1999).

[27] A. Andronic, P. Braun-Munzinger and J. Stachel, Nucl. Phys. A **772**, 167 (2006).

[28] F. Karsch, K. Redlich and A. Tawfik, Phys. Lett. B **571**, 67 (2003)

[29] F. Karsch [RBC Collaboration and HotQCD Collaboration], J. Phys. G **35**, 104096 (2008)

[30] R. Gupta [for the HotQCD Collaboration], PoS 170 (LAT2008), arXiv:0810.1764 [hep-lat].

[31] B. Stokic, B. Friman and K. Redlich, arXiv:0809.3129 [hep-ph].

[32] U. M. Heller, F. Karsch and B. Sturm, Phys. Rev. D **60**, 114502 (1999).

[33] R. V. Gavai, Nucl. Phys. Proc. Suppl. **119**, 529 (2003).

[34] C. R. Allton *et al.*, Phys. Rev. D **68**, 014507 (2003).